Medicinal Chemistry Research (2019) 28:2088–2098
https://doi.org/10.1007/s00044-019-02438-x

MEDICINAL
CHEMISTRY
RESEARCH

ORIGINAL RESEARCH

Aryl azide-sulfonamide hybrids induce cellular apoptosis: synthesis and preliminary screening of their cytotoxicity in human HCT116 and A549 cancer cell lines

Ahmed El-Kardocy[1] · **Muhamad Mustafa**[2] · **Esam R. Ahmed**[3] · **Samy Mohamady**[4] · **Yaser A. Mostafa**[5]

Received: 17 May 2019 / Accepted: 4 September 2019 / Published online: 13 September 2019

Abstract

Simple, small, drug-like molecules bearing aryl azide and aryl sulfonamide moieties were designed and synthesized. The cytotoxic activity of these compounds was measured on colon cancer HCT116, lung cancer A549, and normal fibroblast cells F180 cell lines. All the synthesized compounds showed a significant cytotoxic activity below 100 µM in both HCT116 and A549 cells. Compounds **10e** and **10f** exhibited the most potent activity with IC_{50} values of 2.20 and 6.27 µM on A549 and HCT116 cells, respectively. Also, compounds **10e** and **10f** showed significant tumor selectivity on HCT116 and A549 cell lines when compared with the reference cytotoxic agent staurosporine. This indicated the promising safety of these compounds on normal cells. In addition, flow cytometry studies showed that HCT116 cell lines treated with the most active compound **10f** were arrested in the G2/M phase of the cell cycle. **10f** boosted both early and late apoptosis at HCT116 cells. A hypothetical pharmacophore model was built using 14 reported potent carbonic anhydrase I inhibitors. The pharmacophoric study revealed that the tested sulfonamide derivatives **10e** and **10f** showed significant fitting on the pharmacophore query with reasonable RMSD values. Molecular docking study showed a chelation reaction with the key Zn atom, in addition to different hydrogen bonding, and van der Waals interactions with several important amino acids inside the CA I active site.

Graphical Abstract

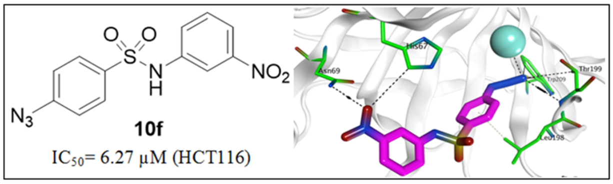

Keywords Sulfonamides · Cytotoxicity · Carbonic anhydrase · Molecular docking · Pharmacophoric study

---

✉ Yaser A. Mostafa
y3abdelh@uwaterloo.ca

[1] Student Research Center, Faculty of Pharmacy, Assiut University, Assiut 71515, Egypt

[2] Pharmaceutical Chemistry Department, Faculty of Pharmacy, Deraya University, Minya, Egypt

[3] VACSERA, Cairo, Egypt

[4] Faculty of Pharmacy, The British University in Egypt, Cairo-Suez Desert Road, Al-Sherouk 11837, Egypt

[5] Pharmaceutical Organic Chemistry Department, Faculty of Pharmacy, Assiut University, Assiut 71526, Egypt

Introduction

It is well known that cancer cells respond to cancer therapeutics through three complexed processes including induction of apoptosis, regulation of cell cycle, and DNA damage-repair processes (Hoeijmakers 2009). Despite a large number of protocols used for the treatment of cancer, there are still few tumor cells able to resist cancer therapeutics leading to therapy impairment or even tumor rebound. Unfortunately, using high doses of cancer therapeutics to overcome such impairment or rebound resulted in emerging severe or even life-threatening side effects (El-Awady et al. 2016). Carbonic anhydrases (CAs) are one of the metalloenzymes that are ubiquitously expressed in the human body. CAs are zinc enzymes that catalyze the reversible hydration of carbon dioxide to bicarbonate and a proton. This simple reaction is crucial for several physiological mechanisms either desirable such as electrolyte secretion, bone resorption, pH regulation, biosynthetic reactions, and calcification which need HCO_3 as a substrate or undesirable such as tumorigenesis. The CA isozymes are found to be interesting therapeutic targets where their inhibition could be utilized to treat a variety of diseases including cancer, oxidative stress, epilepsy, edema, and osteoporosis (Salmon et al. 2012; Gulcin and Beydemir 2013; Carradori et al. 2015; Huang et al. 2017; Bruno et al. 2016). Human CAs I and II are cytosolic enzymes that are prevalent throughout the human body (Arslan et al. 2002). Moreover, CAs IX and XII are human-associated CA isoforms, which are having an extracellular active site, they were found to be a marker for many hypoxic tumors (Barathova et al. 2008; Gondi et al. 2013). Interestingly, literature survey revealed that the vast majority of CAs inhibitors were characterized by being small molecules with promising anticancer activities. Moreover, several studies revealed that there are three major classes of carbonic anhydrase inhibitors (CAIs): sulfonamides, coumarins, and polyamines (Riafrecha et al. 2014). Since the discovery of the sulfonamide inhibitors of CA isozymes, several powerful inhibitors of CAs were designed and synthesized with a common structural pharmacophore, which is the presence of an aromatic or heteroaromatic sulfonamide moiety (Gokcen et al. 2016; Eldehna et al. 2017). Also, several sulfonamide containing compounds were found to possess potent anticancer and CA inhibitory activity, compounds **1–3** (Fig. 1) (Salmon et al. 2012; Arslan et al. 2002; Alaoui et al. 2017; Bagheri et al. 2014; Jain et al. 2010; Prasanna Kumar et al. 2014; El-Din et al. 2015). Moreover, the literature survey showed that aryl azides **4–6** were widely used as the foremost scaffold to design and synthesize novel compounds with antiproliferative activity (Fig. 2) (Tanabe et al. 2012; Nicolaus et al. 2010; da Cruz et al. 2016; Thamilarasan et al. 2015; Lipeeva et al. 2015; Legigan et al. 2012; Pinney et al. 2000; Fu et al. 2017; Spletstoser et al. 2004).

The importance and the remarkable existence of CAs in various sorts of tumors, and the induction of apoptosis by aryl azides made them an excellent target for developing new drug-like small molecules. Hence it is crucial to discover new successful candidates as therapeutics for the treatment of cancer. In the present work, new azide-sulfonamide hybrids (**10a–f**) were designed and synthesized Scheme 1. The sulfonamide derivatives were preliminarily tested and evaluated for their cytotoxic activity against two different cancer cell lines; colon cancer (HCT116) and non-small cell lung cancer (A549) cells, which were deliberately preferred because CA isozymes were found to be notably expressed in colon cancer and lung cancer (Bekku et al. 2000; Wang et al. 2016). Moreover, flow cytometry and cell cycle analysis were implemented on the most active derivatives. In addition, for defining the potential mechanism of action, the most active derivatives were chosen for fitting on the pharmacophoric query and extensive docking studies.

Results and discussion

Chemistry

The synthesis of target compounds **(10a–f)** is outlined in Scheme 1. The key intermediate **9** was obtained after four

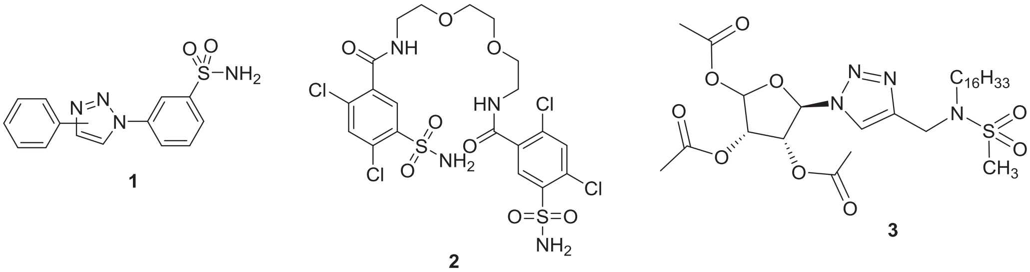

Fig. 1 Chemical structures of carbonic anhydrase inhibitors containing sulfonamide moiety

Fig. 2 Chemical structures of aryl azide derivatives possessing anti-proliferative activity

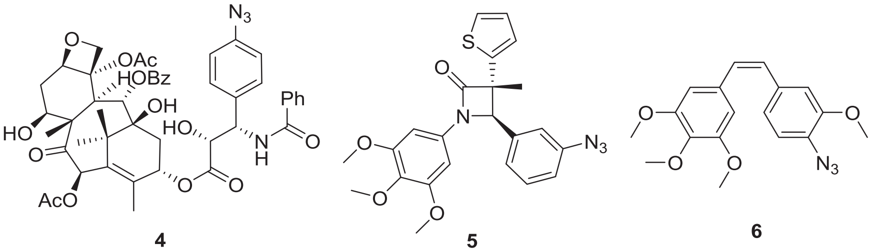

4 5 6

Scheme 1 Synthetic approach of compounds (**10a–f**). I Na_2CO_3, $NaNO_2$, HCl, 0–5 °C; II (**a**) NaN_3; (**b**) $SOCl_2$, DMF, heat; III appropriate aniline, Pyridine, rt, 16 h

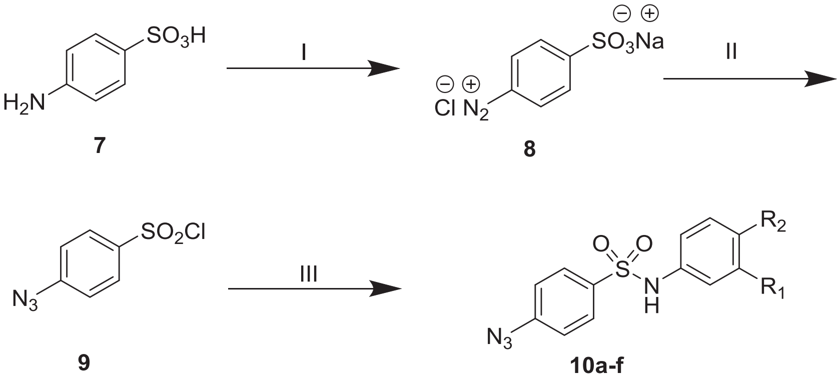

7 8 9 10a-f

Table 1 IC_{50} (μM) values for the tested compounds against colon cancer cells (HCT116), lung cancer cells (A594), normal human fibroblast cells (F180), and tumor selectivity (TS)

			IC_{50} (μM)				
Compound	R_1	R_2	HCT116 (A)	A549 (B)	F180 (C)	TS_1 (C)/(A)	TS_2 (C)/(B)
10a	H	H	13.48 ± 0.44	39.21 ± 1.18	17.22 ± 0.29	1.28	0.44
10b	H	Br	28.66 ± 0.94	7.31 ± 0.22	39.32 ± 1.18	1.37	5.38
10c	H	Cl	11.48 ± 0.37	12.07 ± 0.42	15.26 ± 0.55	1.33	1.26
10d	H	OCH_3	34.96 ± 1.15	16.37 ± 0.52	37.85 ± 0.63	1.08	2.31
10e	H	NO_2	52.99 ± 1.74	2.20 ± 0.07	53.90 ± 0.18	1.02	24.5
10f	NO_2	H	6.27 ± 0.20	34.59 ± 0.93	54.52 ± 1.27	8.69	1.57
			Positive control				
Staurosporine			7.92 ± 0.26	10.55 ± 0.34	8.26 ± 0.16	1.04	0.78

IC_{50} resembles the concentration required to inhibit tumor growth by 50%

steps with a high yield (76%) without further purification. The detailed synthesis procedures, as well as the characterization data, are represented in the experimental part. The target sulfonamides **(10a–f)** were synthesized in a moderate to a high yield from the main intermediate **9** upon its reaction with different anilines in presence of pyridine as a solvent at room temperature (Table 1). The ^{1}H NMR spectra of compounds **(10a–f)** revealed a common broad signal of sulfonamide group NH; around 10.30 ± 0.2 ppm except for the two nitro derivatives, Compounds **10e** and **10f**, which were downfield shifted to 10.91 ppm because of the strong electron-withdrawing effect of the nitro group. In addition, the ^{13}C NMR spectra of the sulfonamides **(10a–f)** displayed common signals around 128 and 121 ppm corresponding to CHs of *p*-azido-benzene sulfonamide aromatic ring. The C, H, N, and S microanalyses of all synthesized compounds were determined and were within ±0.4 of theoretical values.

Biological investigation

In vitro cytotoxic activities

In vitro cytotoxic activity of the synthesized sulfonamides **10a–f** was tested using the MTT assay on the viability of two different human cancer cells (colon cancer HCT116 and non-small cell lung cancer A549 cell lines (Table 1). Staurosporine served as a positive control. Because it is a matter of concentration dependence, the percentages of viable cells declined substantially upon increasing the concentrations of the sulfonamide derivatives. After 48 h of incubation, cell viability was analyzed at five different concentrations of 100, 25, 6.25, 1.56, and 0.39 µM. The HCT116 cell viability was ~73% at a concentration of 0.39 µM when treated with the *m*-NO_2 sulfonamide derivative **10f** (black), the viability percentages significantly lessened upon increasing the concentration to reach 28% at 100 µM (Fig. 3). Compared with the synthesized sulfonamides, **10f** showed the highest ability to inhibit HCT116 growth with an IC_{50} value of 6.26 µM, while the reference staurosporine showed an IC_{50} value of 9.92 µM. While the sulfonamide derivatives **10a** (red) and **10c** (green) exhibited a remarkable drop in the viability percentages from about 74 and 81% at 0.39 µM to 35 and 30% at 100 µM, respectively. **10a** and **10c** showed IC_{50} values of about 1.7–1.5-folds lower in the inhibitory activity than the reference staurosporine, respectively. Regarding A549 cell lines, **10e** (orange) effectively decreased cell viability from 61% at a concentration of 0.39 µM to 29% at 100 µM (Fig. 4). The *p*-NO_2 sulfonamide **10e** exhibited an IC_{50} value of 2.20 µM, which is markedly lower than that of Staurosporine (IC_{50} = 10.55 µM). Moreover, the *p*-Br sulfonamide derivative **10b** significantly lessened cell viability from 70% at a concentration of 0.39 µM to 35% at 100 µM. **10b** showed an IC_{50} value of 7.31 µM which is also better than that of staurosporine. Furthermore, compounds **10c** and **10d** showed comparable inhibitory activity to staurosporine with IC_{50} values of 12.07 and 16.36 µM, respectively. Compounds **10f** and **10a** were less active in comparison to their congeners or even to the reference compound on A549 cells with IC_{50} values of 34.59 and 39.21 µM, respectively.

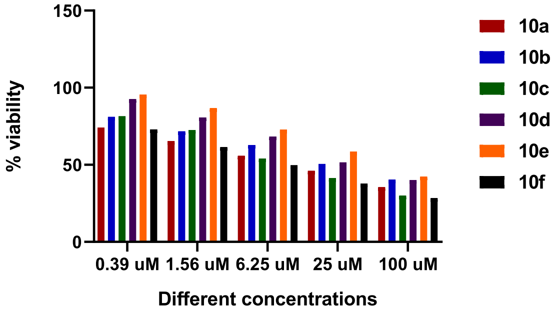

Fig. 3 Effect of the sulfonamide derivatives (**10a–f**) on viability of HCT116 colon cancer cells

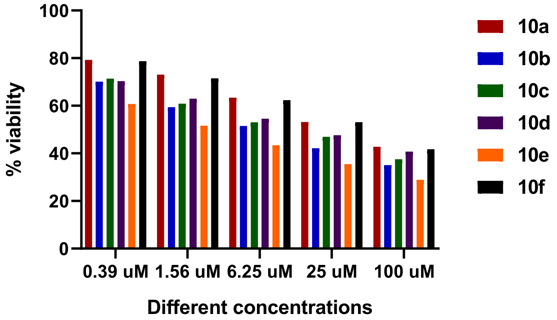

Fig. 4 Effect of the sulfonamide derivatives (**10a–f**) on viability of A549 lung cancer cells

In vitro cytotoxicity towards normal F180 cells

Cytotoxic activities of the synthesized sulfonamides were tested on the non-tumor normal fibroblast cells F180 (Table 1). Selective cytotoxicity is the main problem of anticancer drugs in the market. Subsequently, if the compound has selectivity towards cancer cells, that compound will inevitably be evaluated as a possible anticancer drug candidate for further experiments. To investigate whether the prepared compounds have such selectivity or not, tumor selectivity (TS) values were calculated. First TS (TS_1) calculations were performed by dividing the IC_{50} values towards normal cells F180 to the IC_{50} values towards HCT116 cancer cells (TS_1 = column C/column A) (Table 1). Second TS (TS_2) calculations were made by dividing the IC_{50} values towards normal cells F180 to the IC_{50} values towards A549 cancer cells (TS_2 = column B/column A). When the calculated TS values were compared with that of the reference drug, it was obvious that the tested compounds were more selective towards cancer cells than staurosporine. Compound **10f** was eight times more selective towards HCT116 cancer cells than staurosporine. Also, the sulfonamide **10e** was 31-fold more selective towards A549 cancer cells than the reference drug. These strong findings revealed that these two potent sulfonamides have high selectivity towards cancer cell lines which could be used as possible anticancer drug candidates.

Cell cycle analysis by flow cytometry

Apoptosis induction represents one of the most successful approaches for the development of cancer therapy (Hu and Kavanagh 2003). In addition, several sulfonamide containing compounds were found to induce apoptosis and arrest cell cycle at different phases (Sabt et al. 2018; Bagheri et al. 2014). Consequently, cell cycle analysis was performed on HCT116 cells for **10f** to determine whether the cytotoxic activity resulted from arresting the cell cycle. The *m*-NO_2 sulfonamide **10f** which possessed the best IC_{50} concentration and showed the best TS on HCT116 cancer cells, affected significantly the cell cycle distribution at its IC_{50} value (6.26 µM). The results showed that the cells treated with **10f** induced a significant growth arrest at G2/M phase (Fig. 5). Compared with 6.13% for the untreated HCT116 cells, compound **10f** arrested 26.45% of the cells (Table 2). Moreover, **10f** induced pre-G1 apoptotic cell death with 13.54% compared with the negative control cells which showed only 1.39%. These results showed that the

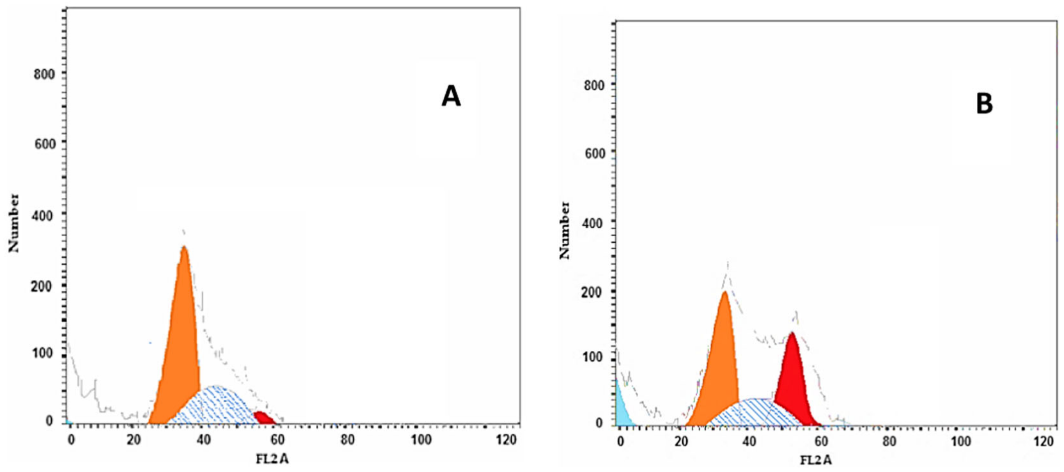

Fig. 5 Cell cycle analysis of HCT116 cells treated with Annexin PI; **a** Untreated cells, **b** cells treated with **10f**

Table 2 Percentages of arresting cell cycle at different phases

Compound	G0-G1	S	G2/M	Pre-G1
Control	49.75	44.12	6.13	1.39
10f	37.26	36.29	26.45	13.54

sulfonamide derivative **10f** was able to arrest cells at G2/M phase and to induce apoptosis.

Induction of cellular apoptosis

The active compound **10f** was tested for its potency to induce apoptosis in HCT116 cell lines by staining with Annexin V-FITC and propodium iodide. After treatment with its IC_{50} concentration, the obtained data showed a considerable ability of **10f** to initiate cellular apoptosis and to disperse cellular integrity (Fig. 6). **10f** elevated the percentage of early apoptotic cells up to 6.49% compared with 0.76% of the negative control (the lower right quadrant). Furthermore, **10f** dispersed cellular integrity by raising the percentage of late apoptotic cells to 5.33%, while the negative control possessed only 0.27% (the upper right quadrant). These results implied that the sulfonamide derivative exhibited most of its cytotoxicity by inducing cellular apoptosis.

Pharmacophore modeling

A pharmacophoric model was created to affirm the CA I inhibitory mechanism of the synthesized compounds. The pharmacophore query was performed using a training set of 14 reported active CA I inhibitors. The most active derivative was selected from each series (Bulut et al. 2017; Turkan et al. 2019; Yıldırım et al. 2015; Gulçin et al. 2017; Gul et al. 2016; Kocyigit et al. 2016, 2017; Gul et al. 2017; Taslimi et al. 2016; Ceylan et al. 2017; Budak et al. 2017; Mete et al. 2016; Boztas et al. 2014; Kucukoglu et al. 2016). The model included hydrophobic domain (Hyd), aromatic center domain (Aro), hydrogen bond acceptors domain (Acc), hydrogen bond donor domain (Don), charged or ionizable groups (Cat & Ani), and/or metal ligator domain (ML) united together with geometrical constraints, such as distances, angles, and dihedral angles. The most active compounds **10e** and **10f** were selected for the pharmacophore study. The tested compounds **10e** and **10f** showed good fitting in the pharmacophoric query with remarkable RMSD values of 7.336 and 0.7307, respectively.

The initial pharmacophoric query was executed and it was formed of five features, as given in Table 3 and demonstrated graphically in Fig. 7a. The tested sulfonamide derivatives **10e** and **10f** showed complete fitting on the query (Fig. 7b, c, respectively) compared with the reference acetazolamide (Fig. 7d). This emphasized the remarkable CAI inhibitory activity of the synthesized compounds. Also, the pharmacophore model revealed the ability of the azide group to interact with Zn atom inside the CA active site.

Molecular docking study

To rationalize the significant effect of the synthesized sulfonamides, molecular modeling was performed to illustrate the interactions of the most active compounds within the CA I binding site. The docked compounds showed coordinate bonds with zinc atom Table 4. Moreover, several hydrogen-bonding interactions and pi-interactions were observed with key amino acids. Strong hydrophobic interactions were further observed with

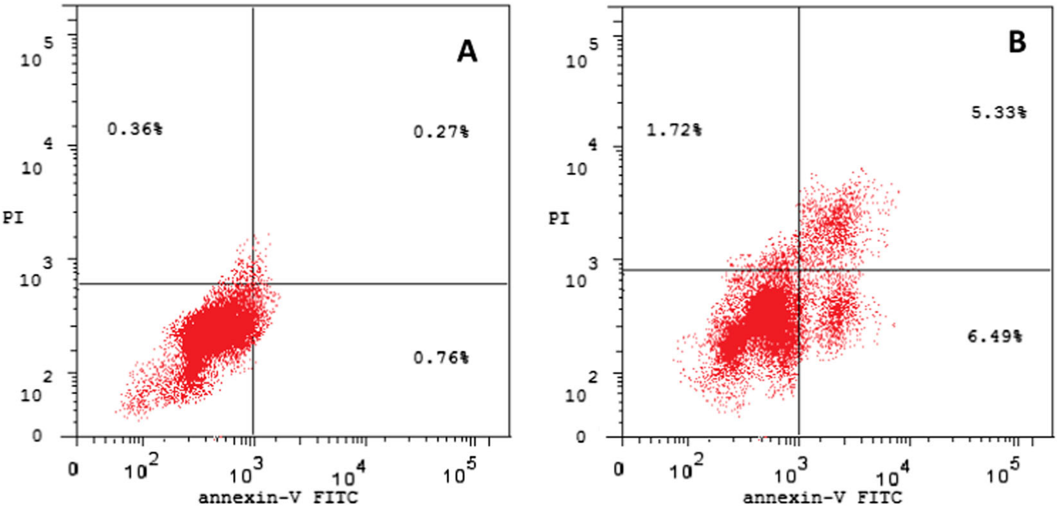

Fig. 6 Contour diagram of Annexin V/PI flow cytometry: **a** Untreated cells, **b** cells treated with **10f**

Table 3 Pharmacophoric and structure features of the training set

Pharmacophoric features	Structural features
F1: Aro/Hyd	Substituted phenyl group
F2: Aro/Hyd	Substituted phenyl group
F3: (Acc/Don/ML)	SO_2NH
F4: (Acc/ML)	Azide group
F5: (Acc/ML)	Azide group

Leu131, Asn69, His67, His200, phe91, Gln92, and Leu198. The binding mode of **10e** (cyan) which exhibited the best inhibitory activity on A549 cells, showed a coordinate bond between the azide nitrogen and zinc atom with interaction energy of −0.5 kcal/mol (Fig. 8). Also, the azide group showed a hydrogen bond with Thr199 (−1.2 kcal/mol). The sulfonamide oxygen showed a hydrogen bond with His67 (−1.4 kcal/mol). The role of the *p*-niro group was observed by forming a hydrogen bond with Ala132 with interaction energy of −0.3 kcal/mol. Moreover, several hydrophobic interactions were observed with Phe91, His94, Pro202, Ala135, Lue198, and Leu131 amino acids. Compound **10f** (magenta) which possessed the best cytotoxic activity on HCT116 cells, showed a coordinate bond between zinc atom and the azide group with interaction energy of −0.3 kcal/mol (Fig. 9). Also, the azide group made additional interactions showing two hydrogen bonds with Thr199 and Trp209 amino acids. The nitro group served as a hydrogen bond acceptor with His67 and Asn69 (−0.2 and −1.4 kcal/mol, respectively). H–pi interaction was observed between the phenyl sulfonamide ring and Leu198. **10f** showed several hydrophobic interactions with Gln92, His200, Asn69, Leu198, and Phe91 amino acids.

Conclusion

In conclusion, we reported the cytotoxic effects of certain new azidosulfonamide derivatives in colon cancer cells (HCT116), lung cancer cells (A549), and normal fibroblast cells (F180). Compounds **10e** and **10f** showed significant cytotoxic effects in both A549 and HCT116 ($IC_{50} = 2.20$ and 6.26 μM, respectively), with powerful TS values. Preliminary mode of action studies revealed that compound **10f** halted cell cycle progression at G2/M phase and induced apoptosis in HCT116 cells. Pharmacophoric features were recognized and the prepared compounds revealed a remarkable fitting on the created model. Molecular docking study showed a higher fitting of **10e** and **10f** on CAI active site. This would warrants additional testing in the in vivo cancer models.

Materials and methods

Chemistry

All starting materials and reagents were obtained from Alpha Aesar Chemical Company and Sigma-Aldrich Chemicals Company. Pyridine was distilled from KOH pellets, thionyl chloride was freshly distilled under reduced pressure, and toluene was distilled over CaH under reduced pressure. Silica gel chromatography was performed using silica gel obtained from Fluka^{TM}. Most of ^1H and ^{13}C spectra were recorded on a JEOL ECA-500 II spectrometer. For NMR spectra obtained using DMSO-d_6 as the solvent, chemical shifts (δ) for ^1H NMR spectra are reported relative to internal Me_4Si (δ 0.0 ppm), and chemical shifts for ^{13}C spectra are relative to the residual solvent peak (δ 39.5 ppm,

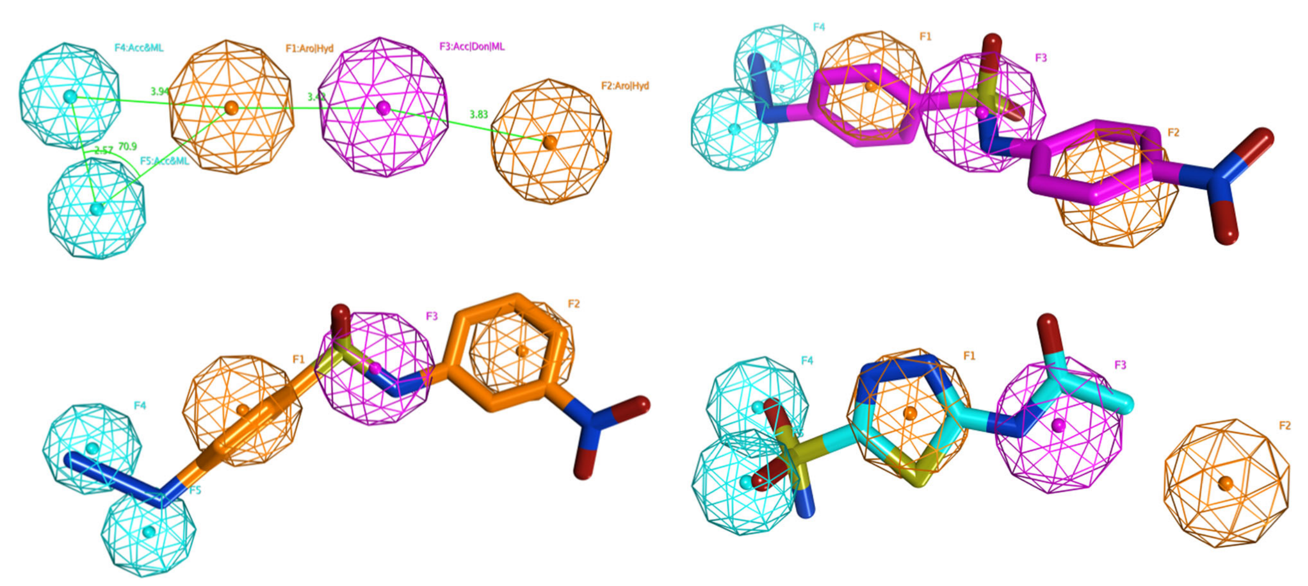

Fig. 7 **a** Pharmacophoric query showing pharmacophoric features, **b** fitting of **10e** to pharmacophore query, **c** fitting of **10f** to pharmacophore query, and **d** fitting of the reference compounds acetazolamide

Table 4 Energy scores (kcal/mol) and binding features for the top potent compounds **10e** and **10f** with carbonic anhydrase I binding site

Compound	Energy score (S) (kcal/mol)	Ligand-receptor interactions		
		Residue	Type	Length (Å)
10e	−4.57	Zn	Coordinate bond	3.13
		Thr199	Hydrogen bond	3.91
		Ala132	Hydrogen bond	3.68
		His67	Hydrogen bond	3.28
		Zn	Coordinate bond	3.15
10f	−4.15	Thr199	Hydrogen bond	3.29
		Trp209	Hydrogen bond	3.75
		Asn69	Hydrogen bond	3.26
		His67	Hydrogen bond	3.75
		Leu198	H–Pi	3.70

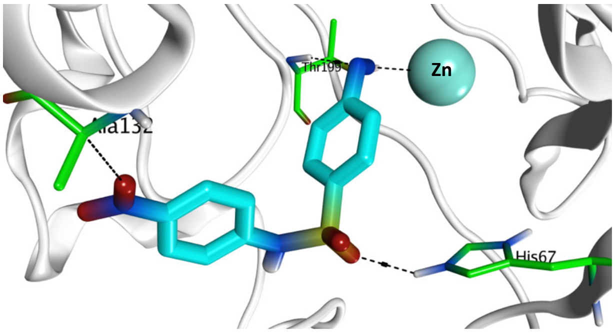

Fig. 8 Docking pose of **10e** (cyan) with CAI active site (PDB code: 4WR7)

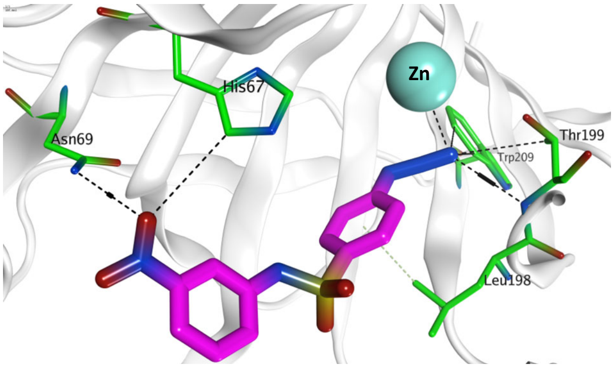

Fig. 9 Docking pose of **10f** (magenta) with CAI active site (PDB code: 4WR7)

central peak). Microanalyses, determined for C, H, and other elements, were within ± 0.4 of theoretical values. Melting points were determined on a Fisher-Johns melting point apparatus and are uncorrected.

Synthesis of 4-azidobenezenesulfonyl chloride 9

To a solution of sodium carbonate (5.8 g) in H_2O (200 ml), sulfanilic acid **7** (250 g) was added portion-wise with vigorous stirring. To the resultant solution, sodium nitrite (8.4 g) was added and stirring was continued till complete dissolution of sodium nitrite. This step was followed by a portion-wise addition of a solution of concentrated HCl (14 mL) in H_2O (30 ml) with vigorous stirring in ice bath to maintain reaction between 0 and 5 °C. A white precipitate was obtained **8**, separated by suction and washed with about 80 ml of cold water. The precipitate solid was then dispersed in 40 ml of cold water, whereupon a solution of sodium azide (8 g in 20 ml water) was added portion-wise till evolution of N_2 ceased. After that sodium chloride (30 g) was added to salt out. The resulting precipitate was filtered off and dried in vacuum to yield a yellowish-white precipitate. 5 g of the resultant azido derivative was dissolved in thionyl chloride (20 ml) and three drops of DMF and heated till boiling for 30 min. After completion of the reaction, the excess thionyl chloride was removed under vacuum and residue was extracted with diethyl ether (100 ml). The etherial extract was evaporated under vacuum to afford 4-azidobenzene sulfonyl chloride **9** as a yellowish-white solid (4.1 g, 76%). mp 59–61 °C; ^{1}H NMR (DMSO-d_6, 500 MHz) δ 7.04–7.07 (m, 2H, Ar–H), 7.60–7.63 (m, 2H, Ar–H); ^{13}C NMR(DMSO-d_6, 125 MHz) δ 144.9, 139.5, 127.5 ($2CH_{Ar}$), 118.4 ($2CH_{Ar}$).

General procedure for synthesis of 4-azido-(un)substituted-phenyl-benzenesulfonamides, compounds 10a–f

To a solution of **9** (0.01 mmol), appropriate anilines were added (0.01 mmol) in dry pyridine (1 ml) at 0 °C. After addition, the reaction was stirred for 16 h at room temperature, and then pyridine was azeotropically removed with toluene under vacuum. The residue was dissolved in ethyl acetate, washed with water and brine, and then dried with Na_2SO_4, filtered, and concentrated under vacuum.

4-Azido-phenyl-benzenesulfonamide 10a Purification was achieved using flash chromatography (ethyl acetate/hexane, 3:7) which provided **10a** as a faint buff solid (78%). mp 94–96 °C (Mirian et al. 2011); ^{1}H NMR (DMSO-d_6, 500 MHz), δ 10.36 (brs, 1H, $SO_2N\underline{H}$), 8.14 (app. dd, 2H, $J = 2.5$ and 2 Hz, Ar–H), 7.91 (app. t, 2H, $J = 2$ and 7 Hz, Ar–H), 7.22 (app. dd, $J = 5$ and 7 Hz, 2H, Ar–H); 7.17–7.04 (m, 2H, Ar–H), 6.59–6.57 (m, 1H, Ar–H); ^{13}C NMR (DMSO-d_6, 125 MHz) δ 145.1, 143.8, 138, 128.9 ($2CH_{Ar}$), 126.5 ($2CH_{Ar}$), 120.1 ($2CH_{Ar}$), 118.3 (CH_{Ar}), 116.0 ($2CH_{Ar}$). Anal. Calcd. for $C_{12}H_{10}N_4O_2S$ (274.0524): C, 52.54; H, 3.67; N, 20.43; S, 11.69; Found: C, 52.31; H, 3.90; N, 20.65; and S, 11.47.

4-Azido-4-bromophenyl-benzenesulfonamide 10b Purification was achieved using flash chromatography (ethyl acetate/hexane, 4:6) which provided **10b** as a brown solid (66%). mp 112–114 °C; ^{1}H NMR (DMSO-d_6, 500 MHz), δ 10.44 (s, 1H, $SO_2N\underline{H}$), 7.73 (app. dd, $J = 2.5$ and 8.5 Hz, 2H, Ar–H), 7.41 (m, 2H, Ar–H), 7.25 (m, 2H, Ar–H), 7.03 (apparent ddd, $J = 2$, 2.5 and 4.5 Hz, 2H, Ar-H); ^{13}C NMR (DMSO-d_6, 125 MHz) δ 144.3, 137.0, 135.1, 132.1 ($2CH_{Ar}$), 128.7 ($2CH_{Ar}$), 121.9 ($2CH_{Ar}$), 119.9 ($2CH_{Ar}$), 116.3; Anal. Calcd. for $C_{12}H_9BrN_4O_2S$ (351.963): C, 40.81; H, 2.57; N, 15.86; S, 9.08; Found: C, 41.90; H, 2.84; N, 15.73; and S, 9.21.

4-Azido-4-chlorophenyl-benzenesulfonamide 10c Purification was achieved using flash chromatography (ethyl acetate/hexane, 4:6) which provided **10c** as a buff solid (71%). mp 122–124 °C; ^{1}H NMR (DMSO-d_6, 500 MHz), δ 10.42 (s, 1H, $–SO_2N\underline{H}$), 7.73 (app. ddd, $J = 2$, 3 and 5 Hz, 2H, Ar–H), 7.30–7.24 (m, 4H, Ar–H), 7.08 (m, 2H, Ar–H); ^{13}C NMR (DMSO-d_6, 125 MHz) δ 144.3, 136.6, 135.1, 129.2 ($2CH_{Ar}$), 128.7 ($2CH_{Ar}$), 128.3, 121.7 ($2CH_{Ar}$), 119.9 ($2CH_{Ar}$); Anal. Calcd. for $C_{12}H_9ClN_4O_2S$ (308.0135): C, 46.68; H, 2.94; N, 18.15; S, 10.39 Found: C, 47.04; H, 3.17; N, 18.41; and S, 10.20.

4-Azido-4-methoxyphenyl-benzenesulfonamide 10d Purification was achieved using flash chromatography (ethyl acetate/hexane, 3:7) which provided **10d** as a white solid (63%). mp 74–75 °C (Mirian et al. 2011); ^{1}H NMR (DMSO-d_6, 500 MHz), δ 10.15 (s, 1H, $SO_2N\underline{H}$), 7.77 (app. dd, $J = 2$ & 4 Hz, 2H, Ar–H), 7.68–7.65 (m, 2H, Ar–H), 6.99 (m, 2H, Ar–H), 6.75 (m, 2H, Ar–H), 3.80 (s, 3H, OCH_3); ^{13}C NMR (DMSO-d_6, 125 MHz) δ 149.9, 144.3, 136.6, 135.1, 129.2 ($2CH_{Ar}$), 128 ($2CH_{Ar}$), 121.7 ($2\ CH_{Ar}$), 115.9 ($2CH_{Ar}$); Anal. Calcd. for $C_{13}H_{12}N_4O_3S$ (304.063): C, 51.31; H, 3.97; N, 18.41; S, 10.54; Found: C, 51.09; H, 3.89; N, 18.63; and S, 10.48.

4-Azido-4-nitrophenyl-benzenesulfonamide 10e Purification was achieved using flash chromatography (ethyl acetate/hexane, 1:9) which provided **10e** as a yellow solid (81%). mp 104–105 °C; ^{1}H NMR (DMSO-d_6, 500 MHz), δ 10.93 (s, 1H, $SO_2N\underline{H}$), 8.12–8.10 (m, 2H, Ar–H), 7.93–7.84 (m, 2H, Ar–H), 7.27 (m, 2H, Ar–H), 6.58 (app. dd, $J = 2$ and 5.5 Hz, 2H, Ar–H); ^{13}C NMR (DMSO-d_6, 125 MHz) δ 155.8, 144.9, 142.2, 142.7, 128.9 ($2CH_{Ar}$), 126.5 ($2CH_{Ar}$), 120.3 ($2CH_{Ar}$), 112.5 ($2CH_{Ar}$). Anal. Calcd. for $C_{12}H_9N_5O_4S$ (319.0375): C, 45.14; H, 2.84; N, 21.93; S, 10.04; Found: C, 45.39; H, 2.97; N, 22.23; and S, 9.89.

4-Azido-3-nitrophenyl-benzenesulfonamide 10f Purification was achieved using flash chromatography (ethyl acetate/hexane, 1:9) which provided **10f** as a yellow solid (76%). mp 98–100 °C; ^{1}H NMR (DMSO-d_6, 500 MHz), δ 10.93 (s, 1H, $SO_2N\underline{H}$), 7.92 (app. t, $J = 2.5$ Hz, 1H, Ar–H), 7.88–7.86 (m, 1H, Ar–H), 7.80–7.78 (m, 1H, Ar–H), 7.55–7.49 (m, 2H, Ar–H), 7.28–7.23 (m, 3H, Ar–H); ^{13}C NMR (DMSO-d_6, 125 MHz) δ 150.1, 148.2, 144.8, 139, 130.9, 128.8 ($2CH_{Ar}$), 125.5, 120.1 ($2CH_{Ar}$), 109.9, 107.1 (C_{Ar}); Anal. Calcd. for $C_{12}H_9N_5O_4S$ (319.0375): C, 45.14; H, 2.84; N, 21.93; S, 10.04; Found: C, 45.43; H, 3.06; N, 22.07; and S, 9.93.

Biology

Cell culture

The pure cultures of A549 (ATCC® CCL-185) (Lung cancer cell line) and HCT116 (ATCC® CCL-247) (Colon cancer cell line) were obtained from (ATCC®) American Type Culture Collection, F180 (normal fibroblast cells) was obtained from VACSERA. The cells were grown and maintained in DMEM (Dulbecco's Modified Eagle's Medium -ATCC® 30-2002), supplemented with 10% FBS (HyClone™), 10 µg/ml Insulin (Sigma®), and 1% penicillin-streptomycin to prevent the bacterial contamination and incubated at 37 °C in a humidified atmosphere having 5% CO_2 for 24 h. The entire plate was observed after 24 h of treatment in an inverted phase-contrast tissue culture microscope, and after treatment of cells with serial concentrations of the compound to be tested in DMSO was incubated for 48 h at 37°C, and then plates were examined and processed for the MTT assay.

MTT assay for in vitro cytotoxicity

The MTT method of monitoring in vitro cytotoxicity is well suited for use with multiwell plates. The sample content in the wells was removed after 48 h of the incubation period and reconstitutes each vial of MTT (M-5655) to be used with 3 ml of medium or balanced salt solution without phenol red and serum. Add reconstituted MTT in an amount equal to 10% of the culture medium volume. Return cultures to the incubator for 2–4 h depending on cell type and maximum cell density. An incubation period of 2 h is generally adequate but may be lengthened for low cell densities or cells with lower metabolic activity. The supernatant was then removed and an equal amount of MTT solubilization solution (M-8910; DMSO), Sigma-Aldrich, USA) was added, and then the wells were mixed (in a gyratory shaker) in order to enhance solubilization of the insoluble formazan crystals. The cells were subjected to different treatments after 24 h of seeding. The cells were then incubated for 48 h with staurosporine as a positive control, test drugs or vehicle (DMSO). Spectrophotometrically measurement of absorbance at a wavelength of 570 nm using Microplate reader, and the percentage viability was calculated by using the formula: % Cell viability = [(OD of treated)/(OD of control)] × 100, the plot of % cell viability versus log concentrations was used to calculate the concentration of compounds in micromoles which reduce the viable cell number of by 50% (IC_{50}).

Cell cycle analysis (assessment of apoptosis)

The apoptotic effect of synthesized azido sulfonamides, Compounds **(10a–f)**, was analyzed by ab139418 Propidium iodide (PI) Flow Cytometry Kit for cell cycle analysis (Annexin V Apoptosis Detection Kit®) according to the manufacturer's instructions. Data analysis and nuclear morphology of apoptotic cells were examined using BD FACS Calibur. PI histograms of normal and treated cells with the cell count on the *y*-axis and the PI fluorescence intensity on the *x*-axis were recorded. Also, the cell cycle arrest caused by compounds **(10a–f)** in a concentration-dependent manner in HCT116 cells was examined.

Pharmacophore study

Pharmacophore modeling and visualization processes were performed using Molecular Operating Environment (MOE) 2014.09 software (Chemical Computing Group, Montreal, QC, Canada). The database of the most active CA I inhibitors was collected. The energy of the structures was minimized using MMF94FX forcefield with gradient RMS of 0.001 kcal/mol. Structures were aligned. The energy cutoff was 10 kcal/mol, while the conformational search was stochastic. The radius of the created pharmacophoric features were from 1.2–1.5 Å. The lowest RMSD values were selected for every compound in the pharmacophoric database

Docking study

Molecular modeling and visualization processes were performed within the CA I active site using MOE 2014.09 software (Chemical Computing Group, Montreal, QC, Canada). The co-crystal structure was retrieved from the RCSB Protein Data Bank (PDB code 4WR7). The compounds were prepared with the standard protocol designated in MOE 2014.09. The energy of the docked structures was minimized using MMF94FX forcefield with gradient RMS of 0.001 kcal/mol. then the protein structure was prepared by using the MOE LigX protocol. To validate the docking study at the CA I active site, the native ligand acetazolamide was re-docked into the binding site using the same set of parameters as described above. The RMSD of the best-docked pose was 0.6243 Å, thus validating the docking using MOE. The ligands were then docked in the binding site using the triangle matcher placement method. Refinement was carried out using Forcefield and scored using the Affinity dG scoring system. The resulting docking poses were visually inspected, and the pose of the lowest binding free energy value was considered.

Acknowledgements The authors extend their appreciation to faculty of Pharmacy, the British University in Egypt and the Pharmaceutical Organic Chemistry Department, Faculty of Pharmacy, Assiut University for their support to synthesis these azide-sulfonamides and perform the preliminary cytotoxic studies. Special thanks to Assoc. Prof. Ahmed S. Aboraia for helping in performing the pharmacophoric study.

Compliance with ethical standards

Conflict of interest The authors declare that they have no conflict of interest.

Publisher's note Springer Nature remains neutral with regard to jurisdictional claims in published maps and institutional affiliations.

References

Alaoui S, Dufies M, Driowya M, Demange L, Bougrin K, Robert G et al. (2017) Synthesis and anti-cancer activities of new sulfonamides 4-substituted-triazolyl nucleosides. Bioorg Med Chem Lett 27(9):1989–1992

Arslan O, Çakir Ü, Uğraş H (2002) Synthesis of new sulfonamide inhibitors of carbonic anhydrase. Biochemistry 67(9):1055–1057

Bagheri F, Safarian S, Eslaminejad MB, Sheibani N (2014) Stable overexpression of DNA fragmentation factor in T-47D cells: sensitization of breast cancer cells to apoptosis in response to acetazolamide and sulfabenzamide. Mol Biol Rep 41 (11):7387–7394. https://doi.org/10.1007/s11033-014-3626-3

Barathova M, Takacova M, Holotnakova T, Gibadulinova A, Ohradanova A, Zatovicova M et al. (2008) Alternative splicing variant of the hypoxia marker carbonic anhydrase IX expressed independently of hypoxia and tumour phenotype. Br J Cancer 98 (1):129

Bekku S, Mochizuki H, Yamamoto T, Ueno H, Takayama E, Tadakuma T (2000) Expression of carbonic anhydrase I or II and correlation to clinical aspects of colorectal cancer. Hepato-Gastroenterology 47(34):998–1001

Boztas M, Cetinkaya Y, Topal M, Gulcin I, Menzek A, Sahin E et al. (2014) Synthesis and carbonic anhydrase isoenzymes I, II, IX, and XII inhibitory effects of dimethoxybromophenol derivatives incorporating cyclopropane moieties. J Med Chem 58 (2):640–650

Bruno E, Buemi MR, De Luca L, Ferro S, Monforte AM, Supuran CT et al. (2016) In vivo evaluation of selective carbonic anhydrase inhibitors as potential anticonvulsant agents. ChemMedChem 11 (16):1812–1818

Budak Y, Kocyigit UM, Gürdere MB, Özcan K, Taslimi P, Gülçin İ et al. (2017) Synthesis and investigation of antibacterial activities and carbonic anhydrase and acetyl cholinesterase inhibition profiles of novel 4,5-dihydropyrazol and pyrazolyl-thiazole derivatives containing methanoisoindol-1,3-dion unit. Synth Commun 47(24):2313–2323

Bulut N, Kocyigit U, Gecibesler I, Dastan T, Karci H, Taslimi P et al. (2017) Synthesis of some novel pyridine compounds containing bis-124-triazole/thiosemicarbazide moiety and investigation of their antioxidant properties carbonic anhydrase and acetylcholinesterase enzymes inhibition profiles. J Biochem Mol Toxicol 32(1):1–10 (e22006)

Carradori S, Mollica A, De Monte C, Granese A, Supuran C (2015) Nitric oxide donors and selective carbonic anhydrase inhibitors: a dual pharmacological approach for the treatment of glaucoma, cancer and osteoporosis. Molecules 20(4):5667–5679

Ceylan M, Kocyigit UM, Usta NC, Gürbüzlü B, Temel Y, Alwasel SH et al. (2017) Synthesis, carbonic anhydrase I and II isoenzymes inhibition properties, and antibacterial activities of novel tetralone-based 1,4-benzothiazepine derivatives. J Biochem Mol Toxicol 31(4):e21872

da Cruz EH, Silvers MA, Jardim GA, Resende JM, Cavalcanti BC, Bomfim IS et al. (2016) Synthesis and antitumor activity of selenium-containing quinone-based triazoles possessing two redox centres, and their mechanistic insights. Eur J Med Chem 122:1–16

El-Awady RA, Semreen MH, Saber-Ayad MM, Cyprian F, Menon V, Al-Tel TH (2016) Modulation of DNA damage response and induction of apoptosis mediates synergism between doxorubicin and a new imidazopyridine derivative in breast and lung cancer cells. DNA Repair 37:1–11

El-Din MMG, El-Gamal MI, Abdel-Maksoud MS, Yoo KH, Oh C-H (2015) Synthesis and in vitro antiproliferative activity of new 1,3,4-oxadiazole derivatives possessing sulfonamide moiety. Eur J Med Chem 90:45–52

Eldehna WM, Abo-Ashour MF, Nocentini A, Gratteri P, Eissa IH, Fares M et al. (2017) Novel 4/3-((4-oxo-5-(2-oxoindolin-3-ylidene) thiazolidin-2-ylidene) amino) benzenesulfonamides: synthesis, carbonic anhydrase inhibitory activity, anticancer activity and molecular modelling studies. Eur J Med Chem 139:250–262

Fu D-J, Fu L, Liu Y-C, Wang J-W, Wang Y-Q, Han B-K et al. (2017) Structure-activity relationship studies of β-lactam-azide analogues as orally active antitumor agents targeting the tubulin colchicine site. Sci Rep 7(1):12788

Gokcen T, Gulcin I, Ozturk T, Goren AC (2016) A class of sulfonamides as carbonic anhydrase I and II inhibitors. J Enzym Inhib Med Chem 31(sup2):180–188

Gondi G, Mysliwietz J, Hulikova A, Jen JP, Swietach P, Kremmer E et al. (2013) Antitumor efficacy of a monoclonal antibody that inhibits the activity of cancer-associated carbonic anhydrase XII. Cancer Res 73(21):6494–6503

Gul HI, Mete E, Taslimi P, Gulcin I, Supuran CT (2017) Synthesis, carbonic anhydrase I and II inhibition studies of the 1,3,5-trisubstituted-pyrazolines. J Enzym Inhib Med Chem 32 (1):189–192

Gul HI, Tugrak M, Sakagami H, Taslimi P, Gulcin I, Supuran CT (2016) Synthesis and bioactivity studies on new 4-(3-(4-Substitutedphenyl)-3a,4-dihydro-3 H-indeno [1,2-c] pyrazol-2-yl) benzenesulfonamides. J Enzym Inhib Med Chem 31 (6):1619–1624

Gulçin İ, Abbasova M, Taslimi P, Huyut Z, Safarova L, Sujayev A et al. (2017) Synthesis and biological evaluation of aminomethyl and alkoxymethyl derivatives as carbonic anhydrase, acetylcholinesterase and butyrylcholinesterase inhibitors. J Enzym Inhibi Med Chem 32(1):1174–1182

Gulcin I, Beydemir S (2013) Phenolic compounds as antioxidants: carbonic anhydrase isoenzymes inhibitors. Mini Rev Med Chem 13(3):408–430

Hoeijmakers JH (2009) DNA damage, aging, and cancer. New Engl J Med 361(15):1475–1485

Hu W, Kavanagh JJ (2003) Anticancer therapy targeting the apoptotic pathway. Lancet Oncol 4(12):721–729

Huang Q, Chen R, Lin X, Xiang Z (2017) Efficacy of carbonic anhydrase inhibitors in management of cystoid macular edema in retinitis pigmentosa: a meta-analysis. PLoS ONE 12(10): e0186180

Jain AK, Veerasamy R, Vaidya A, Mourya V, Agrawal RK (2010) QSAR analysis of some novel sulfonamides incorporating 1,3,5-triazine derivatives as carbonic anhydrase inhibitors. Med Chem Res 19(9):1191–1202. https://doi.org/10.1007/s00044-009-9262-0

Kocyigit UM, Aslan ON, Gulcin I, Temel Y, Ceylan M (2016) Synthesis and carbonic anhydrase inhibition of novel 2-(4-(Aryl) thiazole-2-yl)-3a,4,7,7a-tetrahydro-1H-4,7-methanoisoindole-1,3 (2H)-dione derivatives. Arch Pharm 349(12):955–963

Kocyigit UM, Budak Y, Eligüzel F, Taslimi P, Kılıç D, Gulçin İ et al. (2017) Synthesis and carbonic anhydrase inhibition of tetrabromo chalcone derivatives. Arch Pharm 350(12):1700198

Kucukoglu K, Oral F, Aydin T, Yamali C, Algul O, Sakagami H et al. (2016) Synthesis, cytotoxicity and carbonic anhydrase inhibitory activities of new pyrazolines. J Enzym Inhib Med Chem 31 (sup4):20–24

Legigan T, Clarhaut J, Renoux B, Tranoy-Opalinski I, Monvoisin A, Berjeaud J-M et al. (2012) Synthesis and antitumor efficacy of a β-glucuronidase-responsive albumin-binding prodrug of doxorubicin. J Med Chem 55(9):4516–4520

Lipeeva AV, Pokrovsky MA, Baev DS, Shakirov MM, Bagryanskaya IY, Tolstikova TG et al. (2015) Synthesis of 1H-1,2,3-triazole linked aryl (arylamidomethyl)–dihydrofurocoumarin hybrids and analysis of their cytotoxicity. Eur J Med Chem 100:119–128

Mete E, Comez B, Inci Gul H, Gulcin I, Supuran CT (2016) Synthesis and carbonic anhydrase inhibitory activities of new thienyl-substituted pyrazoline benzenesulfonamides. J Enzym Inhib Med Chem 31(sup2):1–5

Mirian M, Zarghi A, Sadeghi S, Tabaraki P, Tavallaee M, Dadrass O et al. (2011) Synthesis and cytotoxic evaluation of some novel sulfonamidederivativesagainst a few human cancer cells. Iran J Pharm Res 10(4):741

Nicolaus N, Zapke J, Riesterer P, Neudörfl JM, Prokop A, Oschkinat H et al. (2010) Azides derived from colchicine and their use in library synthesis: a practical entry to new bioactive derivatives of an old natural drug. ChemMedChem 5(5):661–665

Pinney KG, Mejia MP, Villalobos VM, Rosenquist BE, Pettit GR, Verdier-Pinard P et al. (2000) Synthesis and biological evaluation of aryl azide derivatives of combretastatin A-4 as molecular probes for tubulin. Bioorg Med Chem 8(10):2417–2425

Prasanna Kumar BN, Mohana KN, Mallesha L, Veeresh B (2014) Synthesis and in vitro antiproliferative activity of 2,5-disubstituted-1,3,4-oxadiazoles containing trifluoromethyl benzenesulfonamide moiety. Med Chem Res 23(7):3363–3373. https://doi.org/10.1007/s00044-014-0918-z

Riafrecha LE, Rodríguez OM, Vullo D, Supuran CT, Colinas PA (2014) Attachment of carbohydrates to methoxyaryl moieties leads to highly selective inhibitors of the cancer associated carbonic anhydrase isoforms IX and XII. Bioorg Med Chem 22 (19):5308–5314

Sabt A, Abdelhafez OM, El-Haggar RS, Madkour HM, Eldehna WM, El-Khrisy EE-DA et al. (2018) Novel coumarin-6-sulfonamides as apoptotic anti-proliferative agents: synthesis, in vitro biological evaluation, and QSAR studies. J Enzym Inhib Med Chem 33 (1):1095–1107

Salmon AJ, Williams ML, Wu QK, Morizzi J, Gregg D, Charman SA et al. (2012) Metallocene-based inhibitors of cancer-associated carbonic anhydrase enzymes IX and XII. J Med Chem 55 (11):5506–5517

Spletstoser JT, Flaherty PT, Himes RH, Georg GI (2004) Synthesis and anti-tubulin activity of a 3′-(4-azidophenyl)-3′-dephenylpaclitaxel photoaffinity probe. J Med Chem 47(26):6459–6465

Tanabe K, Ishizaki J, Ando Y, Ito T, Nishimoto S-i (2012) Reductive activation of 5-fluorodeoxyuridine prodrug possessing azide methyl group by hypoxic X-irradiation. Bioorg Med Chem Lett 22(4):1682–1685

Taslimi P, Gulcin I, Ozgeris B, Goksu S, Tumer F, Alwasel SH et al. (2016) The human carbonic anhydrase isoenzymes I and II (hCA I and II) inhibition effects of trimethoxyindane derivatives. J Enzym Inhib Med Chem 31(1):152–157

Thamilarasan V, Jayamani A, Sengottuvelan N (2015) Synthesis, molecular structure, biological properties and molecular docking studies on MnII, CoII and ZnII complexes containing bipyridine–azide ligands. Eur J Med Chem 89:266–278

Turkan F, Cetin A, Taslimi P, Karaman M, Gulçin İ (2019) Synthesis, biological evaluation and molecular docking of novel pyrazole derivatives as potent carbonic anhydrase and acetylcholinesterase inhibitors. Bioorg Chem 86:420–427

Wang D-b, Lu X-k, Zhang X, Li Z-g, Li C-x (2016) Carbonic anhydrase 1 is a promising biomarker for early detection of non-small cell lung cancer. Tumor Biol 37(1):553–559

Yıldırım A, Atmaca U, Keskin A, Topal M, Celik M, Gülçin İ et al. (2015) N-Acylsulfonamides strongly inhibit human carbonic anhydrase isoenzymes I and II. Bioorg Med Chem 23 (10):2598–2605